



Changes of dissolved organic matter following salinity invasion in different seasons in a nitrogen rich tidal reach

Rongrong Xie^{a,b,c,*}, Jiabin Qi^{a,1}, Chengchun Shi^d, Peng Zhang^e, Rulin Wu^a, Jiabing Li^{a,b,c}, Joanna J. Waniek^{f,**}

^a College of Environmental Science and Engineering, Fujian Normal University, Fuzhou 350007, China

^b Key Laboratory of Pollution Control and Resource Recycling of Fujian Province, Fujian Normal University, Fuzhou 350007, China

^c Digital Fujian Environmental Monitoring Internet of Things Laboratory, Fujian Normal University, Fuzhou 350007, China

^d Fujian Provincial Academy of Environmental Sciences, Fuzhou 350013, China

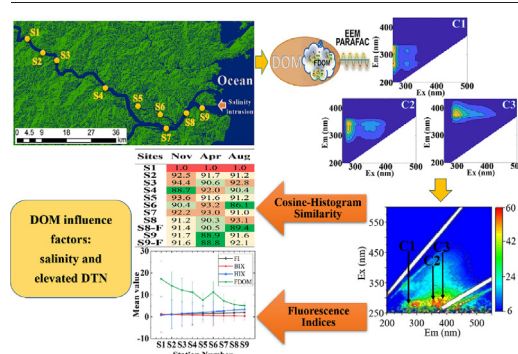
^e School of Environmental and Municipal Engineering, North China University of Water Resources and Electric Power, Zhengzhou 450046, China

^f Leibniz Institute for Baltic Sea Research, Warnemünde, Rostock 18119, Germany

HIGHLIGHTS

- The cosine-histogram similarity was raised to assess the EEM of DOM.
- FI and HIX increased along from upstream to downstream.
- BIX and FDOM decreased generally from upstream to downstream.
- Salinity and elevated DTN significantly affected the DOM.

GRAPHICAL ABSTRACT



ARTICLE INFO

Editor: Frederic Coulon

Keywords:

Tidal reach

DOM

Cosine-histogram similarity

PARAFAC

EEMs

ABSTRACT

Dissolved organic matter (DOM) is a heterogeneous mixture of dissolved material found ubiquitously in aquatic systems and dissolved organic nitrogen is one of its most important components. We hypothesised nitrogen species and salinity intrusions affect the DOM changes. Here, using the nitrogen rich Minjiang River as an easily accessible natural laboratory 3 field surveys with 9 sampling sites (S1-S9) were conducted in November 2018, April and August 2019. The excitation emission matrices (EEMs) of DOM were explored with parallel factor (PARAFAC) and cosine-histogram similarity analysis. Four indices including fluorescence index (FI), biological index (BIX), humification index (HIX) and the fluorescent DOM (FDOM) were calculated and the impact of physicochemical properties was assessed. The results suggested that the highest salinities of 6.15, 2.98 and 10.10, during each campaign corresponded to DTN concentrations of 119.29–240.71, 149.12–262.42 and 88.27–155.29 $\mu\text{mol L}^{-1}$, respectively. PARAFAC analysis revealed the presence of tyrosine-like proteins (C1), tryptophan-like proteins or a combination of the peak N and tryptophan-like fluorophore (C2) and the humic-like material (C3). The EEMs in the upstream reach (i.e. S1-S3) were complex with larger spectra ranges, higher intensities and similar similarity. Subsequently, the fluorescence intensity of three components decreased significantly with low similarity of EEMs (i.e. S4-S7). At the downstream, the fluorescence levels dispersed significantly and no obvious peaks were seen except in August. In addition, FI and HIX increased, while BIX and FDOM decreased from upstream to downstream. The salinity positively correlated with FI

Abbreviations: DOM, Dissolved organic matter; PARAFAC, Parallel factor analysis; EEMs, Excitation emission matrices.

* Correspondence to: R. Xie, 8 Shangsang Rd, Fuzhou 350007, China.

** Correspondence to: J. J. Waniek, 15 Seestraße, Rostock 18119, Germany.

E-mail addresses: xierr1118@163.com (R. Xie), joanna.waniek@io-warnemuende.de (J.J. Waniek).

¹ The authors contributed equally to this work.

<http://dx.doi.org/10.1016/j.scitotenv.2023.163251>

Received 10 February 2023; Received in revised form 26 March 2023; Accepted 30 March 2023

Available online 5 April 2023

0048-9697/© 2023 Elsevier B.V. All rights reserved.

and HIX, and negatively related to BIX and FDOM. Besides, the elevated DTN had a significant effect on the DOM fluorescence indices. Altogether, salinity intrusion and elevated nitrogen are relevant for the distribution of the DOM, which is helpful for the water management tracing the DOM source according to the on-line monitoring of salinity and nitrogen in estuaries.

1. Introduction

Dissolved organic matter (DOM) is a complex and dynamic mixture of molecules that arises from the death and exudation of organisms, and their subsequent decomposition (Berg et al., 2021). In the coastal environments, the DOM pools were from the allochthonous inputs including terrestrial runoff, river discharge and groundwater flushing, and the autochthonous inputs including phytoplankton metabolism and excretion, viral lysis and releases associated with zooplankton grazing (Nagata, 2000; Aitkenhead-Peterson et al., 2003). These different sources varied seasonally and regionally, making the composition of the DOM complex and highly variable. The tidal reach, encompasses freshwater and marine ecosystems, and are highly productive areas (Xie et al., 2020). Most megacities are located at their shores, which are intensively used for recreation, transport and all kind of commercial activities (Adey and Loveland, 2007). Nowadays, a decline in the health of tidal reach has been widely observed due to this continuously growing intensive anthropogenic pressure (Bricker et al., 2008; Kennish, 2016). Salinity intrusion and elevated nitrogen concentrations in estuarine system are growing problems in many cities (Xie et al., 2020; Des et al., 2021). Many studies proved the relationship between DOM and the organic nitrogen in the wastewater (Chen et al., 2011; Czerwionka et al., 2012; Mesfioui et al., 2012; Sirivedhin and Gray, 2005). However, little is known about the relationship between the nitrogen and DOM involved in the response to saltwater intrusion in nitrogen rich aquatic environments.

DOM is a pool of organic molecules of allochthonous and autochthonous origins (Coble, 2007; Murphy et al., 2008; Stedmon et al., 2007) and can be easily transported and transformed because of its heterogeneity (Ogawa et al., 2001; Wen et al., 2022). The allochthonous DOM in aquatic systems is composed of organic carbon, nitrogen, phosphorus and sulfur coming from the terrestrial ecosystem while the autochthonous DOM is from in-situ biological production and more aliphatic (Liu et al., 2020). The allochthonous DOM may drive shifts in community composition, whereas autochthonous DOM seems to affect the community composition transiently. Usually, the allochthonous DOM mixes with the autochthonous DOM at the hyporheic zone where most of the microbial activity takes place (Wagner et al., 2014).

Tremendous progress has been made in the past 30 years towards understanding the biochemical structure of DOM and its role in the biogeochemistry of aquatic ecosystems. Fluorescence has been used to analyze DOM in natural and engineered water bodies (Kalbitz et al., 2000; Zhang et al., 2023). Operationally, the presence of protein-like fluorescent components was indicative of either microbial activity (freshwater) (Stedmon and Markager, 2005; Stedmon et al., 2007) or anthropogenic inputs (wastewater-impacted water) (Goldman et al., 2012). In the Arctic Ocean the growth of algae was found to cause a rise in the intensity of the protein-like fluorescence peaks (Chen et al., 2017), and the biological index increased in the same pace indicating the increase of substances of autochthonous origin. The inter-component interactions of DOM and the input of terrestrial materials played important roles in the photo degradation and biodegradation in rivers (Wang et al., 2015; Song et al., 2022). Meanwhile, the phytoplankton in rivers could produce non-fluorescent organic matter, which then changed to the DOM due to the bacteria action (Fisher and Rochelle-Newall, 2002). Hence, the changes of DOM could depend both on DOM molecules and the aquatic environment itself.

Three-dimensional excitation-emission matrix (EEM) and parallel factor analysis (PARAFAC) have been greatly advanced to characterize the DOM (Stedmon and Bro, 2008; Zhang et al., 2011). EEM fluorescence techniques

provide specific “fingerprints” for a mixture of fluorescent components within a complex matrix (Henderson et al., 2009; Hudson et al., 2008; Peiris et al., 2011) and had been widely used to distinguish between allochthonous and autochthonous DOM sources in aquatic environments (Del Castillo et al., 1999; Mayer et al., 1999). Besides, the location of the fluorescence peaks and the fluorescence intensity in the EEM were affected by the degree of humification as well as by the structural characteristics of the humic macromolecule including carboxylic acid and aromatic structure, which could reveal the composition of the fluorophores in the DOM (Chen et al., 2003a; Rodríguez et al., 2014; Zhang et al., 2008). Five regions including simple aromatic proteins such as tyrosine (Regions I and II), fulvic acid-like materials (Region III), soluble microbial byproduct-like material (Region IV) and humic acid-like organics (Region V) were operationally defined according to the excitation and emission boundaries (Chen et al., 2003b). However, since the EEMs are often composed of various types of overlapping fluorophores, it is difficult to properly evaluate DOM dynamics in coastal areas based solely on the EEM. Therefore, PARAFAC, a statistical modeling approach, was used to decompose the EEM spectra of the end-members and their mixtures (Andersen and Bro, 2003). And then various of fluorescence indices including the fluorescence index (FI), biological index (BIX), humification index (HIX) and the concentration of fluorescent DOM (FDOM) were introduced to access the degree of humification and aromaticity of the DOM according to the specific excitation and emission wavelengths (Rodríguez-Vidal et al., 2020).

The worldwide estuarine areas have been threatened by the sever salinity intrusion and nitrogen pollution. Due to the dual directional flow and downward bottom slope, tidal reaches sustained most of the terrestrial pollutants (Xie et al., 2023). The drastic salinity changes and elevated nitrogen make these systems ideal natural laboratories to study the effects of salinity and nitrogen on changes of DOM. Therefore, three field investigations aimed at answering the question whether salinity and different N forms in a tidal reach alter the distribution and quality of DOM. The physicochemical properties including salinity and N speciation, as well as the DOM were investigated in this study. EEM and PARAFAC methods were used to characterize the DOM, and cosine-histogram similarity theory was used to investigate the regional difference of the pollution sources. Finally, four main fluorescence indices including FI, BIX, HIX and the concentration of FDOM were calculated to assess the impact of physicochemical properties on the DOM (Lin et al., 2023). Our study provides important information for understanding the effect of salinity invasion and high nitrogen levels on the DOM. The results show that on-line salinity and nitrogen monitoring in a nitrogen rich estuarine area could provide technical support for local management agencies for setting up warning system to prevent high DOM concentrations.

2. Materials and methods

2.1. Research area

The Minjiang tidal reach in the south-eastern China was selected as research area (Fig. 1). Minjiang River originates in Jianning County of Fujian Province, and flows into the East China Sea. The tidal reach of Minjiang River, roughly from Shuikou Dam to the Minjiang estuary, is located in a subtropical marine monsoon climate zone. The average annual temperature is 19.7 °C, the average annual number of precipitation days is 153 with annual average precipitation of 1346 mm (Zheng et al., 2006). The Minjiang tidal river is a largely regulated river and the minimum discharge is 308 m³ s⁻¹ (Xie et al., 2017).

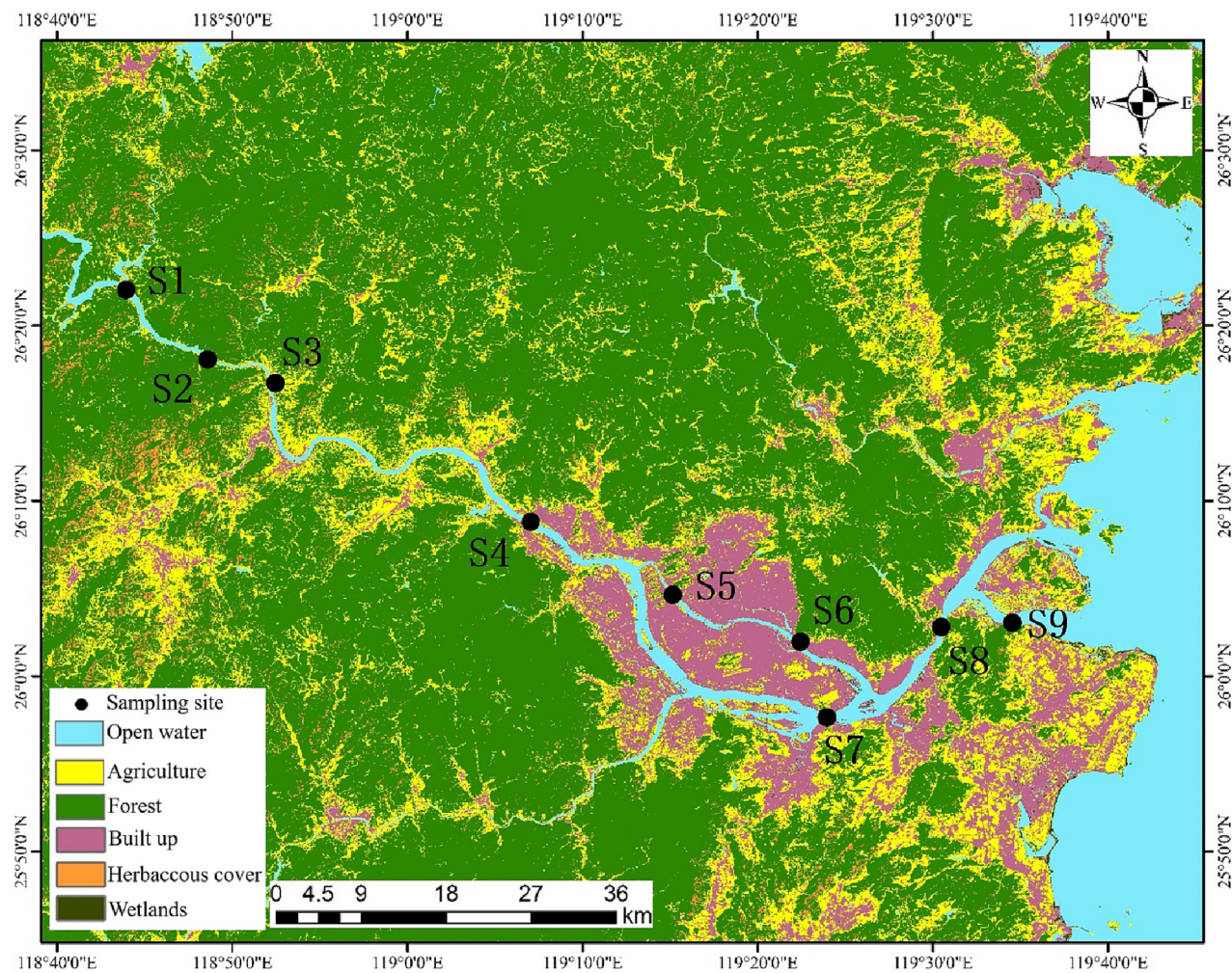


Fig. 1. The Minjing River and sampling sites surveyed (S1-S9).

2.2. Field surveys

2.2.1. Sampling procedures

The river discharge in the research area is depending on weather conditions and the dam regulation. The water quality varied spatially and temporally in response to physical transport processes. Under dry-weather conditions, the NH_4^+ concentration showed variability on tidal scale (DiLorenzo et al., 2004). Hence, three in-field investigations covering

different flow periods were conducted in November 2018 (low-flow period), April 2019 (high-flow period) and September 2019 (mean-flow period). The average discharges of Shuikou dam during the day time (6:00–18:00) was $1189 \text{ m}^3 \text{ s}^{-1}$, $2792 \text{ m}^3 \text{ s}^{-1}$ and $1605 \text{ m}^3 \text{ s}^{-1}$, respectively (Supplementary Fig. S1). In total 9 stations (S1-S9) were occupied to investigate the changes of the DOM in the tidal reach (Fig. 1). Stations S1 and S2 are located in the upstream of the Shuikou Dam and represent the background water quality. While Stations S3-S7 are selected according to the

Table 1
Definition and significance of the DOM optical indices and parameters used in the present study.

Fluorescence indices	Definition and significance	Reference
Fluorescence index: FI	FI is the ratio of emission wavelengths at 450 nm and 500 nm measured at an excitation wavelength of 370 nm. Microbial activity is the main source of DOM for $1.7 < \text{FI} < 2.0$, and the contribution of microbial activity is lower when $\text{FI} < 1.4$.	McKnight et al., 2001; Wickland et al., 2007
Biological index: BIX	BIX is calculated at emission wavelengths 310 nm divided by 430 nm, at excitation wavelength 430 nm. BIX value reflects the ratio of albuminoid and biological components. The values ranging from 0.8 to 1.0 were indicative of freshly produced DOM of biological/microbial origin whereas $\text{BIX} < 0.6$ indicates little amount of organic matter from autochthonous origin.	Huguet et al., 2009; Birdwell and Engel, 2010
Humification index: HIX	HIX is determined as the peak area under the emission spectra for wavelength 435–480 nm divided by those of 300–345 nm, at excitation at 254 nm. HIX value reflects the degree of humification and the complexity of the DOM structure. The low HIX values (< 4) were associated with autochthonous fresh DOM of biological origin or plant biomass and animal manure, whereas high HIX values (> 10) were indicative of strongly humified organic material of terrestrial origin.	Zsolnay et al., 1999; Huguet et al., 2009; Birdwell and Engel, 2010
Concentration of fluorescent DOM: FDOM/R. U.	FDOM is the fraction of chromophoric dissolved organic matter (CDOM) that absorbs UV-Vis and emits fluorescence (Meng et al., 2013; Graeber et al., 2012). $\text{Fn}(355)$ is the maximum of fluorescence intensity ($\text{Em} = 440\text{--}470 \text{ nm}$, at $\text{Ex} = 355 \text{ nm}$) and represents the concentration of FDOM. The $\text{Fn}(355)$ values characterize the content of fluorescent organic substances in natural waters.	Yang et al., 2020

Table 2

The physicochemical properties of water samples in the research area. n was the number of samples, the mean \pm standard deviation and min \sim max in brackets were given.

Index	November 2018		April 2019		August 2019	
	Ebb tide	Flood tide	Ebb tide	Flood tide	Ebb tide	Flood tide
Temperature / °C	21.63 \pm 0.45 (21.90–22.27)	20.92 \pm 0.87 (20.30–21.53)	18.31 \pm 0.68 (17.50–19.90)	17.75 \pm 0.07 (17.70–17.80)	30.34 \pm 0.49 (29.50–31.00)	30.30 \pm 0.71 (29.80–30.80)
pH	7.12 \pm 0.29 (6.80–7.70)	7.60 \pm 0.14 (7.50–7.70)	7.28 \pm 0.26 (6.80–7.70)	7.15 \pm 0.07 (7.10–7.20)	8.01 \pm 0.42 (7.42–8.70)	7.80 \pm 0.28 (7.60–8.00)
Salinity	0.40 \pm 0.99 (0.05–3.05)	3.59 \pm 3.62 (1.03–6.15)	0.03 \pm 0.01 (0.02–0.06)	1.53 \pm 2.05 (0.08–2.98)	0.55 \pm 1.47 (0.03–4.45)	6.42 \pm 5.20 (2.74–10.10)
DO / mg·L ⁻¹	7.04 \pm 0.85 (5.97–8.33)	7.16 \pm 0.49 (6.81–7.50)	6.58 \pm 0.57 (5.60–7.10)	6.55 \pm 1.20 (5.70–7.40)	5.80 \pm 1.75 (3.70–8.09)	6.22 \pm 1.01 (5.50–6.93)
NH ₄ ⁺ / μ mol·L ⁻¹	11.35 \pm 16.47 (0.71–46.43)	1.07 \pm 0.51 (0.71–1.43)	20.94 \pm 4.38 (13.21–26.21)	28.32 \pm 6.82 (23.50–33.14)	25.07 \pm 5.78 (17.84–36.37)	13.69 \pm 0.14 (13.59–13.78)
NO ₃ ⁻ / μ mol·L ⁻¹	98.70 \pm 18.88 (71.57–128.43)	118.21 \pm 16.97 (106.21–130.21)	87.08 \pm 16.70 (72.70–128.25)	87.07 \pm 3.62 (84.51–89.63)	70.50 \pm 22.79 (33.72–118.38)	47.74 \pm 14.34 (37.60–57.88)
DTN / μ mol·L ⁻¹	149.80 \pm 35.24 (119.29–240.71)	155.36 \pm 0.51 (155.00–155.71)	204.23 \pm 31.80 (156.17–262.42)	160.80 \pm 16.52 (149.12–172.49)	121.54 \pm 20.08 (88.27–155.29)	111.21 \pm 11.21 (103.29–119.14)
FI	1.60 \pm 0.22 (1.30–1.97)	1.83 \pm 0.05 (1.79–1.86)	1.37 \pm 0.31 (0.98–1.83)	1.93 \pm 0.08 (1.88–1.98)	1.49 \pm 0.38 (1.02–2.01)	2.06 \pm 0.40 (1.77–2.34)
BIX	0.88 \pm 0.43 (0.35–1.53)	0.43 \pm 0.05 (0.39–0.46)	0.67 \pm 0.22 (0.39–0.92)	0.31 \pm 0.11 (0.23–0.39)	0.71 \pm 0.22 (0.51–1.15)	0.55 \pm 0.02 (0.54–0.57)
HIX	1.89 \pm 0.85 (0.66–2.99)	3.03 \pm 0.04 (3.00–3.06)	2.54 \pm 1.09 (0.87–3.84)	3.84 \pm 0.01 (3.83–3.85)	2.07 \pm 0.76 (0.83–3.10)	3.18 \pm 0.09 (3.12–3.24)
FDOM / R. U.	11.91 \pm 4.76 (6.55–20.45)	6.93 \pm 0.28 (6.73–7.13)	9.88 \pm 3.98 (4.57–16.56)	4.77 \pm 0.68 (4.29–5.24)	8.77 \pm 3.70 (4.12–14.68)	4.14 \pm 0.55 (3.75–4.53)
n	18	4	18	4	18	4

surrounding landscape pattern. Two replicate samples were taken from 0.5 m below the water surface in the midstream during the ebb tide. Furthermore, considering the effect of salinity intrusions samples at stations S8 and S9 were taken. Samples were collected during both the ebb tide and the flood tide, at the lowest (ebb) and highest (flood) water level of each station, respectively, indicating the full effects of freshwater in the upstream or saltwater in the downstream. All samples were taken according to the instructions in ‘Water quality -Technical regulation of the preservation and handling of samples’ (HJ 493, 2009) and subsequently transported to the laboratory. In the lab, the samples were filtered through 0.45 μ m pore size, 50 mm membrane filters (Millipore, Darmstadt, USA) in order to remove large sediment particles, and then were maintained at 0–4 °C. Before analysis, samples were warm up to room temperature.

2.2.2. Physicochemical properties measurement

The salinity, and temperature, pH and dissolved oxygen (DO) were measured on site. The salinity and temperature were monitored using a salinometer (CT-3081, Kedida, China). Water pH and DO were measured using a portable pH meter (IQ 150, IQ Scientific Instruments, San Diego, CA, USA) and a portable dissolved oxygen meter (2010C324-31, JPB-607A, Yidian Scientific Instruments, Ltd., Shanghai, China), respectively. The N speciation (NH₄⁺, NO₃⁻ and DTN) analyses were conducted using standard spectrophotometric methods (UV-1201, Beifen-Ruilia Analytical Instruments, Ltd., Beijing, China) and performed within 7 days after sampling. Briefly, the NH₄⁺, NO₃⁻ and DTN concentrations in the water were determined using Nessler's reagent spectrophotometry (HJ 535, 2009), ultraviolet spectrophotometry (HJ/T 346, 2007) and alkaline potassium persulfate digestion UV spectrophotometry (HJ 636, 2012), respectively. The detection limit of NH₄⁺, NO₃⁻ and DTN was 1.79 μ mol·L⁻¹,

5.71 μ mol·L⁻¹ and 3.57 μ mol·L⁻¹, respectively. All N speciation determinations were carried out in technical duplicates.

2.2.3. EEM measurements and PARAFAC modeling

A single measurement of EEM was made on each sample using a fluorescence spectrophotometer (Hitachi F-7000) with a 700-V xenon lamp. The EEMs were obtained by combining a series of emission scans for wavelength of 250–550 nm and excitation wavelength of 200–500 nm. The excitation and emission slits were set as 5 nm. The scanning speed was 1200 nm/s. The EEMs were Raman calibrated and corrected for excitation and emission instrument biases using the techniques described in Stedmon et al. (2003). The EEM data obtained from the samples in the three surveys were modeled with PARAFAC and each EEM was normalized to the maximum intensity prior to modeling. PARAFAC analysis uses trilinear regression with alternating least squares error minimization to identify the independent components from the complex mixture of DOM fluorophores and trace the changes in the fluorescence intensities:

$$X_{ijk} = \sum_{n=1}^N a_{in} b_{jn} c_{kn} + e_{ijk} \quad (1)$$

where, X_{ijk} is the fluorescence intensity of the i th sample at the k th excitation and j th emission wavelength, a_{in} is directly proportional to the concentration of the n th fluorophore in the i th sample (defined as scores), and b_{jn} and c_{kn} are estimates of the emission and excitation spectrum of the n th fluorophore (defined as loadings), respectively (Stedmon et al., 2003). N is the number of components (individual fluorophore moieties) and e_{ijk} are the residual elements of the model.

The PARAFAC analysis was carried out in MATLAB with the “N-way toolbox for MATLAB” (Andersson and Bro, 2000), and split-half analysis (Stedmon et al., 2003; Cory and McKnight, 2005) was used to validate the identified components.

2.3. Cosine-histogram similarity of EEMs

In this study, we combined the algorithms of cosine similarity and histogram similarity for assessing the similarity of EEMs between S1 and other sampling sites. The fluorescence spectra are expressed as vectors and the cosine distance between each vector is calculated to represent the cosine

Table 3

Pairwise post-hoc test evaluating the significance of possible differences between the sampling months during ebb tide. Significant differences (p -values under 0.05) are bold.

Sampled month groups	R-value	P-value
November 2018/ April 2019	0.403	0.002
November 2018/ August 2019	0.575	0.001
April 2019/ August 2019	0.716	0.001

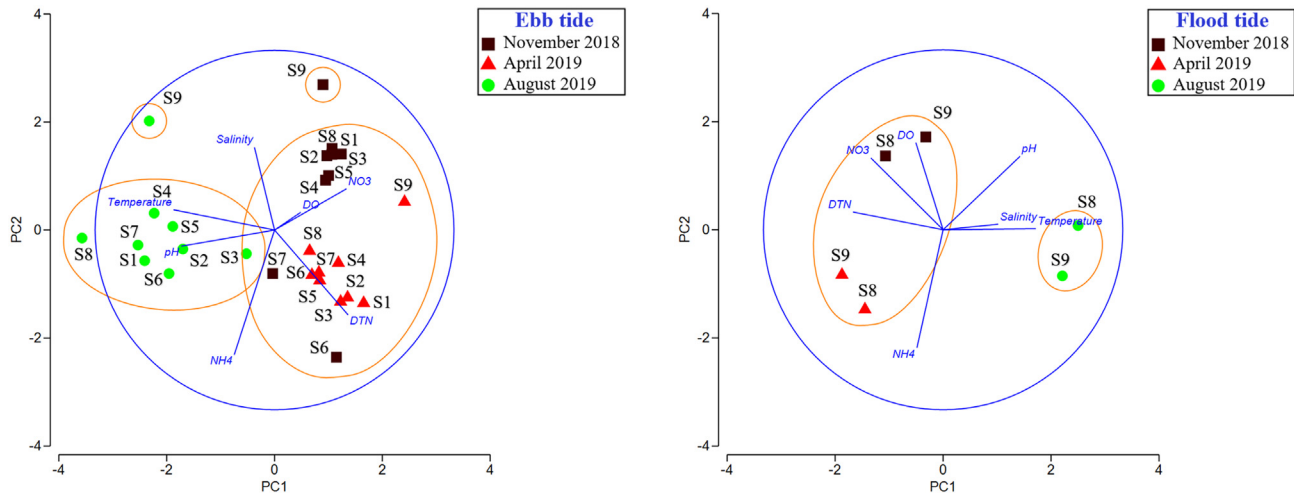


Fig. 2. Principal component analysis (PCA) considering the data collected during the ebb tide and flood tide. Samples classified according to the sampling season (November 2018, April 2019 and August 2019) and the sampling station. Temperature, pH potential of hydrogen, salinity, DO dissolved oxygen, NH_4^+ ammonium, NO_3^- nitrate, DTN dissolved total nitrogen.

similarity of the two spectra. Afterwards the vector colors are compared according to the histogram similarity theory.

Cosine similarity is a measure of similarity between two non-zero vectors (Pesaranghader et al., 2016). Two vectors with the same orientation have a cosine similarity of 1; two vectors at 90° have a similarity of 0. The result of cosine similarity is neatly bounded between 0 and 1. The governing equation is as follows:

$$\text{Cosine_Similarity} = \frac{A \cdot B}{\|A\| \cdot \|B\|} = \frac{\sum_{i=1}^n A_i B_i}{\sqrt{\sum_{i=1}^n A_i^2} \sqrt{\sum_{i=1}^n B_i^2}} \quad (2)$$

where A and B are two fluorescence spectra, respectively.

The level of histogram defines the statistical distribution of the image colors, which are regarded as 8 bit data and the color scale is $2^8 = 256$. The histogram similarity is a measure of color similarity between two images. The same levels of histogram have a similarity of 1, and the similarity of histogram is calculated as follows:

$$\text{Histogram_Similarity}(IMG_1, IMG_2) \triangleq \text{HistSim}(H_1, H_2) = \frac{\sum_{i=0}^{255} \left[1 - \frac{|H_1[i] - H_2[i]|}{\max(H_1[i], H_2[i])} \right]}{256} \quad (3)$$

where let $H_1 = \text{Hist}(IMG_1)$, $H_2 = \text{Hist}(IMG_2)$, H_1, H_2 are the colors of row vectors with 256 elements, and Hist is the histogram operation.

Cosine-histogram similarity was calculated using Python script, and the detailed algorithms are provided in supplementary text 1.

2.4. Fluorescence indices

The description and significance of four fluorescence indices and parameters used in this study are presented in Table 1, which were used to access the degree of humification and aromaticity of the DOM.

2.5. Statistical analyses and graphics

Pairwise tests as post-hoc tests and Principal Component Analysis (PCA) were applied to explore the significance of differences in the concentrations of multiple groups during the three sampling seasons. A cluster analysis was performed to aggregate similar data and facilitate a less subjective interpretation for the PCA. PCA was performed using the PRIMER 7 + PERMANOVA software from PRIMER-e (<https://www.primer-e.com>). The normality test of Shapiro-Wilks and the Levene's variance homogeneity test were applied to the data. The data except NH_4^+ , DO and salinity were normally distributed. Hence, combination of Pearson and Spearman correlation coefficients was used to examine the relationships between fluorescence indices and physicochemical properties.

3. Results and discussion

3.1. Changes in physicochemical properties

The water temperatures during the three seasons were 20.30–22.27 °C, 17.50–19.90 °C and 29.50–31.00 °C, respectively (Table 2). From November 2018 to August 2019, the average pH increased from 7.12 and 7.60 to 8.01 and 7.80 during the ebb tide and flood tide, respectively. An apparent salinity intrusion occurred in November 2018 and August 2019 indicated by salinity of 6.15 and 10.10. While in April with the highest

Table 4

Eigenvalues, variance contribution, accumulated contribution rate of the principal components analysis (PCA) during ebb tide and flood tide.

PC	Ebb tide			Flood tide		
	Eigenvalues	%Variation	Cum.% Variation	Eigenvalues	%Variation	Cum.% Variation
1	2.70	38.6	38.6	3.60	51.4	51.4
2	1.43	20.4	59.0	1.68	24.0	75.4
3	1.13	16.2	75.2	0.94	13.5	88.9
4	0.88	12.6	87.8	0.72	10.3	99.2
5	0.49	7.0	94.8	0.06	0.8	100.0

upstream discharge, the highest salinity was only 2.98. The results indicated the highest salinity in the research area was positive related with the upstream discharge (Xie et al., 2017). Besides, the temperature of seawater could also affect the salinity intrusion, because the higher seawater temperatures significantly increased the tide-induced seawater circulations (Nguyen et al., 2020). Furthermore, the geothermal convection could develop in the regional-scale coastal flow systems, which thereby contributed to the discharge of saline submarine groundwater (Wilson, 2005). The DO concentrations were 5.97–8.33, 5.60–7.40 and 3.70–8.09 $\text{mg}\cdot\text{L}^{-1}$ in November

2018, April 2019, and August 2019, respectively. While the NH_4^+ concentrations were 0.71–46.43, 13.21–33.14 and 13.59–36.37 $\mu\text{mol}\cdot\text{L}^{-1}$, respectively. The concentrations of NO_3^- were 71.57–130.21, 72.70–128.25 and 33.72–118.38 $\mu\text{mol}\cdot\text{L}^{-1}$, respectively. The DTN were, 119.29–240.71, 149.12–262.42 and 88.27–155.29 $\mu\text{mol}\cdot\text{L}^{-1}$, respectively. The nitrogen content was relatively higher in the seasons with lower temperature, caused by the decreased metabolism of microbes under lower temperature conditions (Wen et al., 2021). The average concentrations of DO, NH_4^+ , NO_3^- and DTN had little differences between ebb tide and flood tide

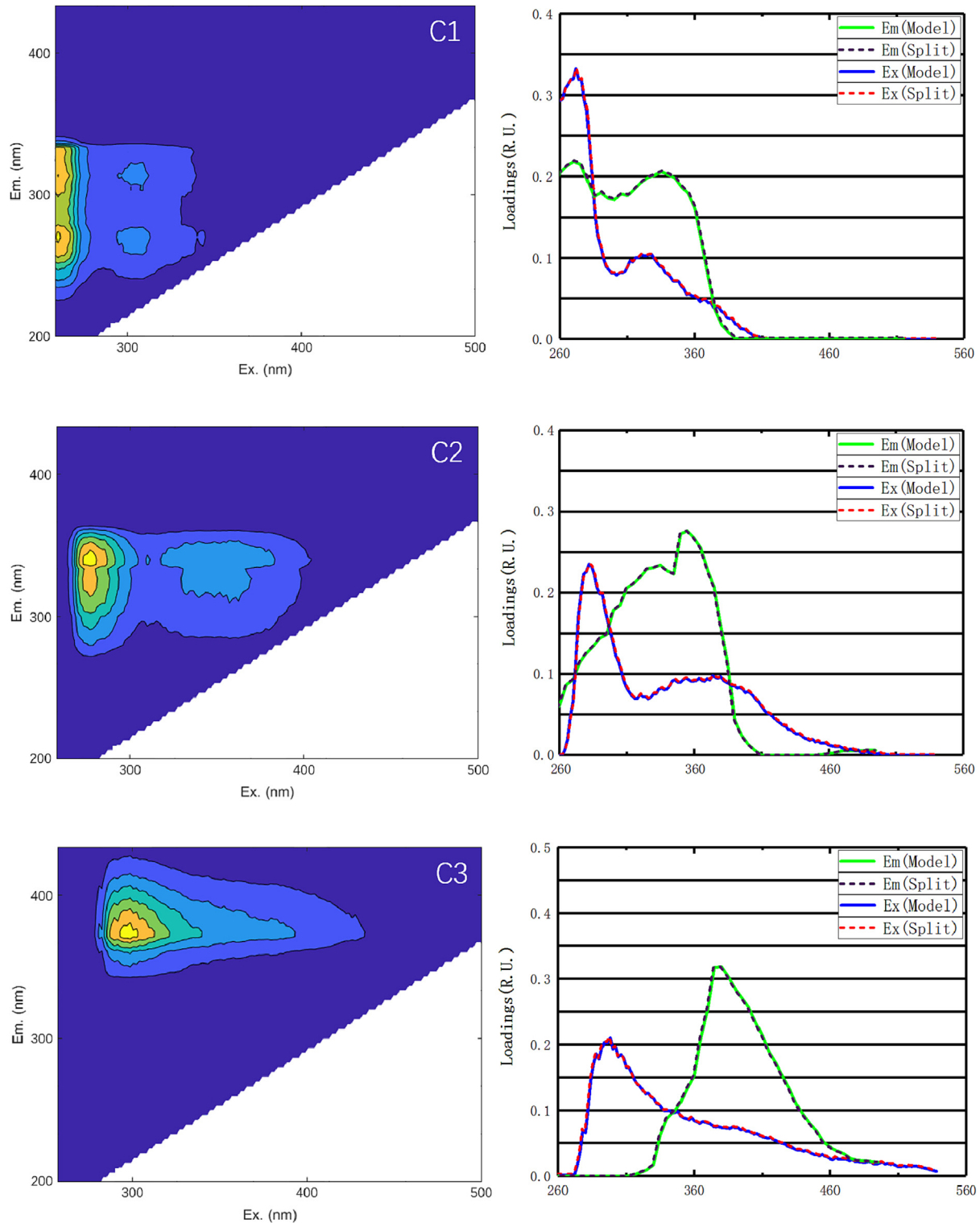


Fig. 3. Contour plots (left) and the excitation/emission loadings (right) of component 1 (top), component 2 (middle) and component 3 (bottom).

(Table 2). The salt intrusion could have a profound impact on aquatic N speciation and transformation processes in tidal river, especially during the flood periods (Xie et al., 2020).

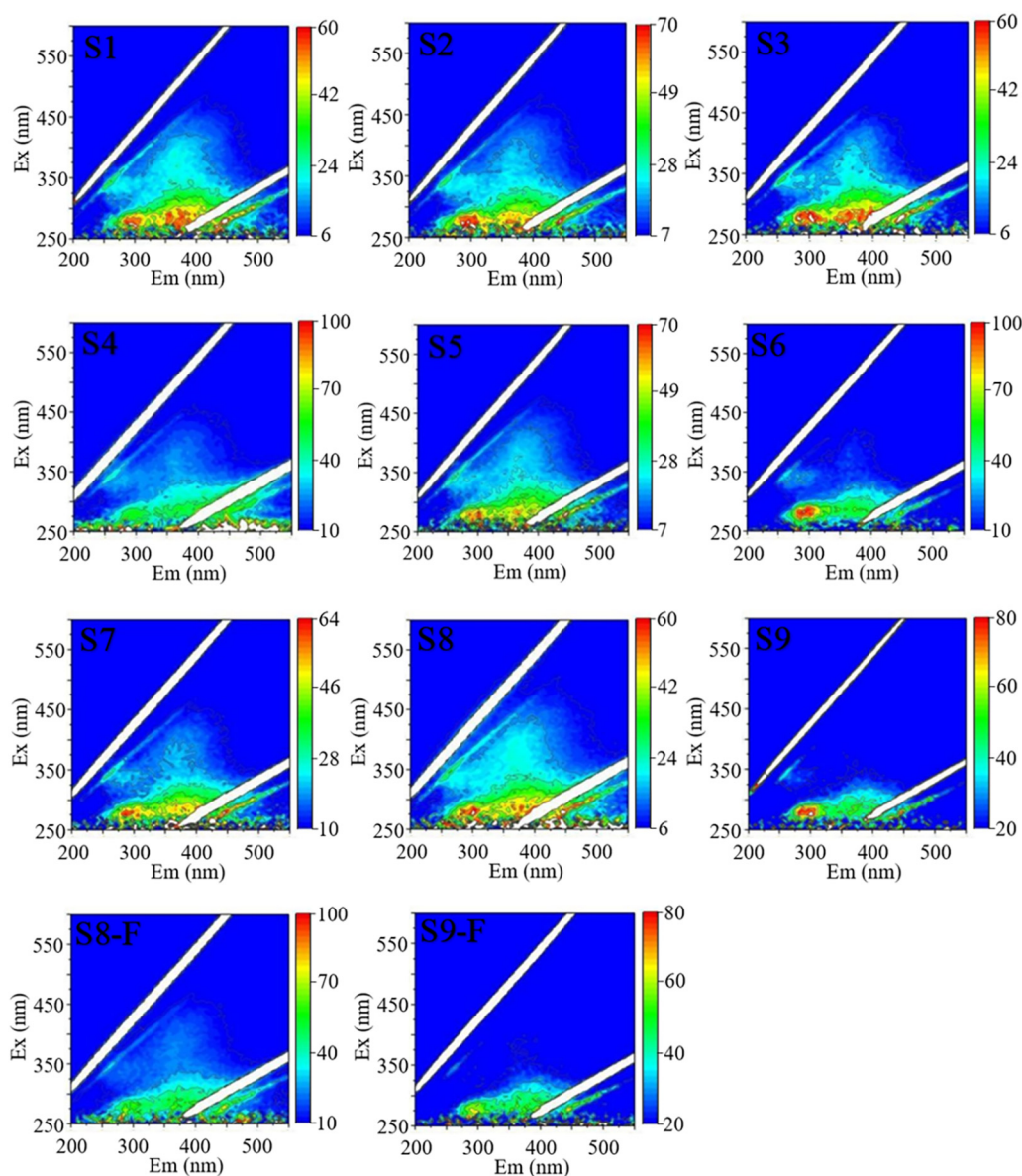
The pairwise post-hoc test, related to the sampled months during the ebb tide, revealed the existence of a clear temporal variability during the ebb tide in a year (Table 3, $p < 0.05$), allowing to conclude that there was a significant difference between the sampled months in all stations. Meanwhile during flood tide the data with only two stations (S8 and S9) were not sufficient for the pairwise post-hoc test. The cluster analysis of the PCAs clearly distinguished between the data collected during the ebb tide and the flood tide (Fig. 2). The results also revealed that the seasonality was the most influencing factor for the physicochemical properties during both the ebb tide and the flood tide in the research area. During the ebb tide and the flood tide, PC2 covered 20.4 % and 24.0 % of the variation existing in the water samples, respectively, with PC1 representing 38.6 % and 51.4 % of this variation (Table 4). A greater dispersion of the data was observed among the sampling stations during the ebb tide, indicating the spatial variability of pollution in the research area (Nascimento et al., 2021). Especially

the highest dispersion occurred at the station S9 due to the mixing of the sea-water and fresh water in the entrance of the estuary (Xie et al., 2023).

3.2. Changes of DOM

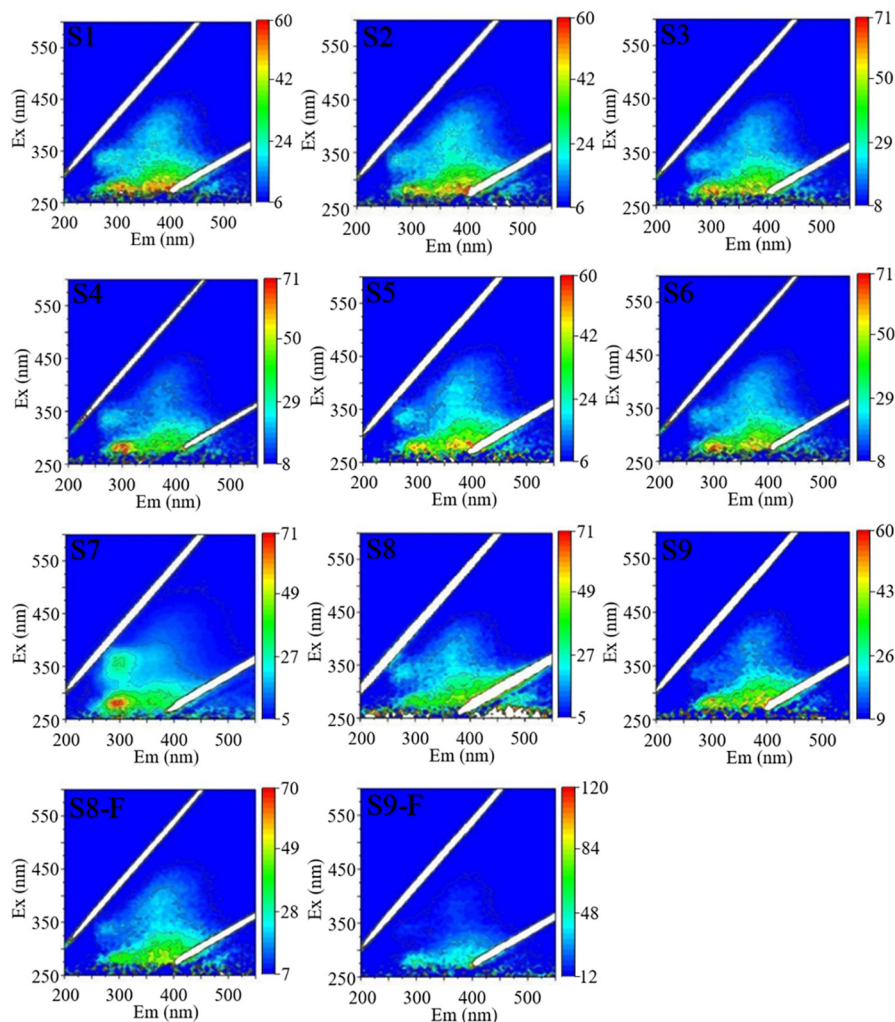
3.2.1. Characteristics of PARAFAC components

Three fluorescent components in the research area were validated according to the PARAFAC analysis. As shown in Fig. 3, component 1 (C1) possessed a primary fluorescence peak at an excitation/emission wavelength pair of 272 nm/270 nm and secondary peak at 272 nm/335 nm. The low excitation wavelength was attributable to tyrosine-like proteins (Meng et al., 2013), which could be attributed to anthropogenically derived organics in waters influenced by wastewater- or plankton-derived organics in fresh waters (Elliott et al., 2006). The peak of component 2 (C2, 282 nm/355 nm) was red shifted compared with C1, which belongs to tryptophan-like proteins or a combination of the peak N and tryptophan-like fluorophore, both of which have been considered to be a labile component produced as a result of biological production in marine



A. November 2018

Fig. 4. Spatiotemporal changes of DOM fluorescence spectra between the ebb tide and the flood tide in the three sampling periods. F stands for the flood tide sample.



B. April 2019

Fig. 4 (continued).

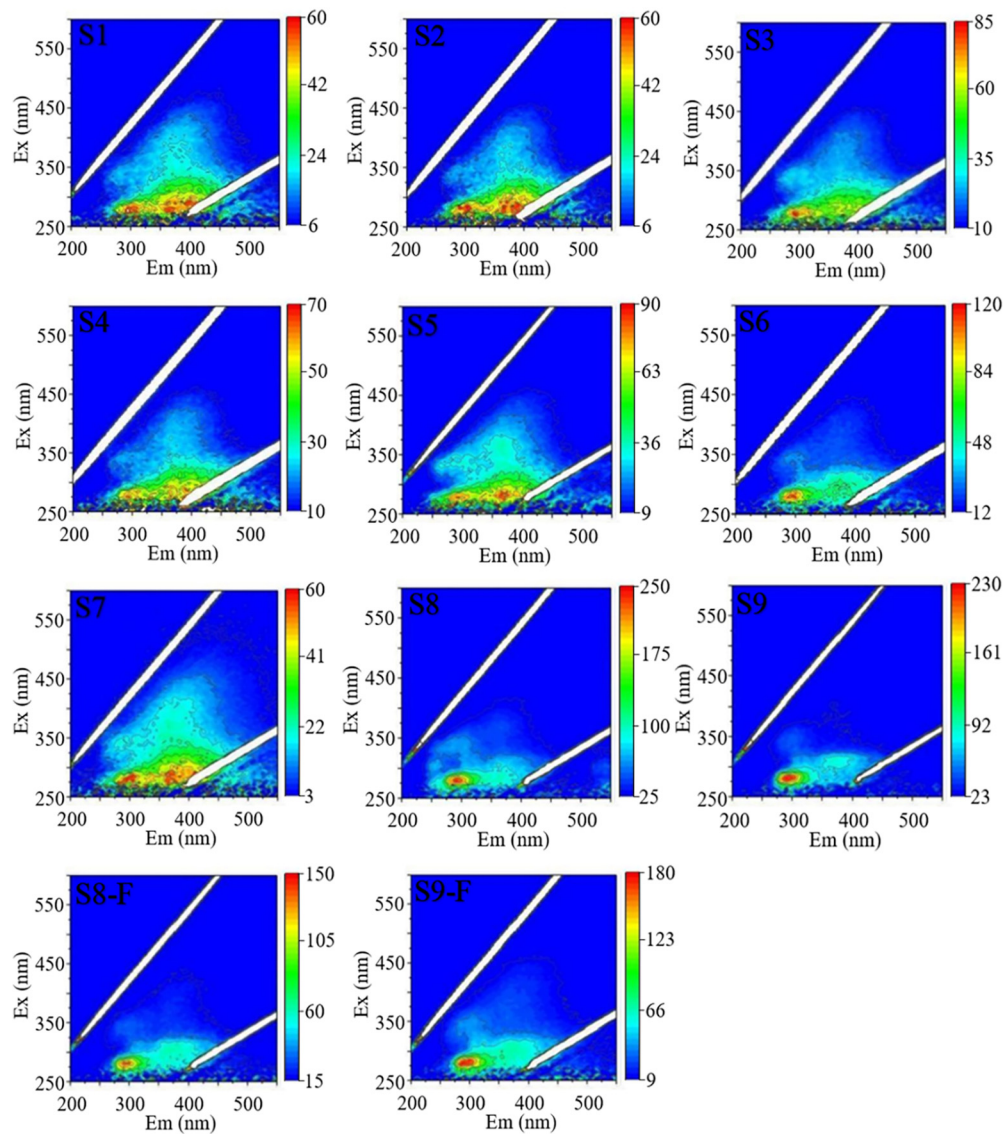
environments (Coble et al., 1998; Yamashita et al., 2008). The peak of components 3 occurred at 298 nm/380 nm and was indicative of the presence of humic-like material (Coble et al., 1998; Chen et al., 2003b; Bridgeman et al., 2011; Wünsch et al., 2019).

3.2.2. Spatiotemporal distribution of the DOM fluorescence spectra

During the three months, the EEMs of DOM in the upstream reach (i.e. stations S1-S3) were quite complex with larger spectra ranges and higher intensities (Fig. 4). The distribution patterns of C1, C2 and C3 were similar in the upstream reach. At station S4, the levels of fluorescence intensity of all components decreased significantly, especially for C2 and C3 in November and April. The decline indicated degradation of DOM due to less exogenous input in the reach. From station S5 to S7 the fluorescence levels showed the local pollution characteristics. All three components appeared at station S5, however the fluorescence levels were weak. C1 dominated the S6 station, which was caused by the freshly produced microbial proteins from the wastewater discharged to the freshwaters and marine/coastal waters (Parlanti et al., 2000; Wu et al., 2003; Zanardi-Lamardo et al., 2004). The S6 had the highest fluorescence intensity in November 2018 because the organic fraction was relatively high during the low-flow period. In addition, the S6 was located at the downstream of the inlet of a city tributary. The microorganisms accumulate more easily in the mixing areas and thereby more metabolites are produced (Wu et al., 2003). Hence, the results for station S6 are more scattered in the

PCA result (Fig. 2). However, at station S7 the fluorescence levels of C2 and C3 decreased from November to the following April and then increased significantly in August. The results confirmed that station S5 was located in drinking water area with strict control of pollution, while stations S6 and S7 were within highly populated areas. At stations S8 and S9, the fluorescence levels dispersed significantly and no obvious peaks were captured, except in August. In the downstream reach of station S8 and S9, the tide took an important impact on the DOM changes. The fluorescence intensities during flood tide decreased in November and April and increased in August respectively compared with those obtained for the ebb tide (Fig. 4).

We have calculated the cosine-histogram similarity of EEMs for the three sampled months to investigate the regional difference of the pollution sources (Table 5). Taking the most complicated EEM of station S1 as the reference object, the similarities between station S1 and the downstream sampling stations in three months were 88.7–94.4, 88.8–93.2 and 86.1–93.1, respectively. The similarities at stations S2 and S3 were relatively close to station S1, except station S3 in April. For stations S4 and S6 the similarities decreased in November and August and increased in April based on the DOM fluorescence intensity. The pollution has different sources at those stations. At station S4 the pollution originates from agriculture land and buildup land, whereas station S6 is located to the downstream of the buildup land (Fig. 1). Besides, the similarities at station S8 and S9 were also different from the similarities calculated for the upstream reach pointing towards the effect of the seawater in this reach during both the



C. August 2019

Fig. 4 (continued).

Table 5
Cosine-histogram similarity of EEMs between station S1 and sampling sites during each sampling period. Red indicated the higher similarity and green indicated the relative low similarity, F indicates samples from flood tide.

Sites	Nov-18	Apr-19	Aug-19
S1	1.0	1.0	1.0
S2	92.5	91.7	91.2
S3	94.4	90.6	92.8
S4	88.7	92.0	90.4
S5	93.6	91.6	91.2
S6	90.4	93.2	86.1
S7	92.2	93.0	91.0
S8	91.2	90.3	93.1
S8-F	91.4	90.5	89.4
S9	91.7	88.9	91.6
S9-F	91.6	88.8	92.1

ebb tide and the flood tide, which was consistent with the salinity invasion pattern and PCA result. The fluorescence levels of stations S8 and S9 were more dispersed in April 2019 because the lower temperature in this month stimulated the production of fresh DOM (Lu et al., 2021). And therefore the similarity were significantly reduced (Table 5). Generally, cosine-histogram similarity of EEMs was similar with the pairwise post-hoc test related to the sampling stations, proving the absence of a clear spatial variability (Supplementary Table S1).

3.3. Changes in DOM fluorescence indices

The FI values ranged from 0.97 to 2.34 and increase significantly from station S1 to S9 (Table 2). The decrease of microbial activity and the consumption of terrestrially derived DOM was considered to be important factors for the increase of FI. FI is typically used to distinguish the sources of DOM (Chu et al., 2022). Our values are similar to ranges reported in previous studies (McKnight et al., 2001). Therefore, we infer that the DOM in the upstream (i.e. stations S1-S2 in November, stations S1-S6 in April and stations S1-S5 in August) derives from terrestrial and allochthonous sources.

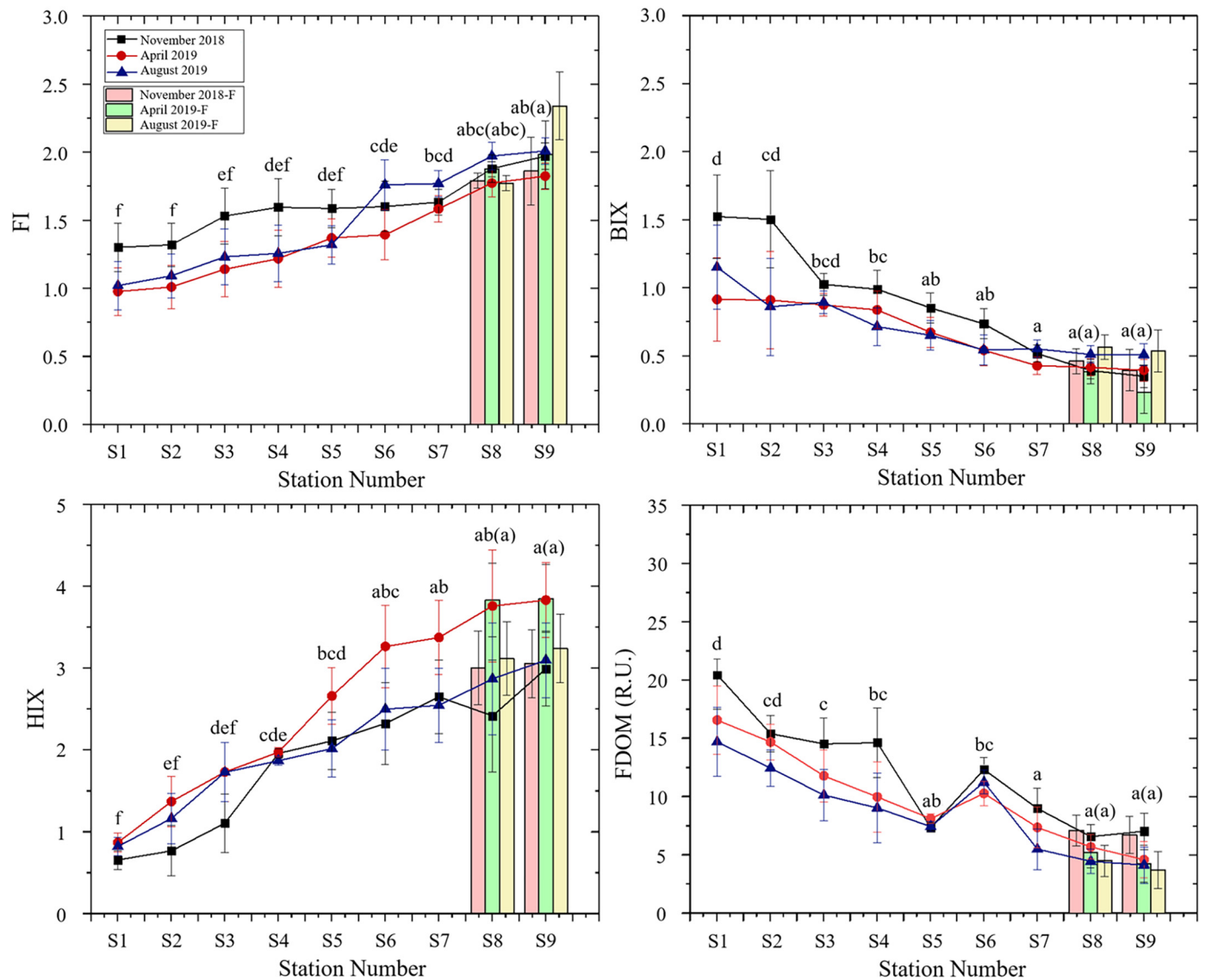


Fig. 5. Spatiotemporal changes of DOM fluorescence indices between ebb tide and flood tide in November 2018, April 2019 and August 2019. F represented the flood tide sample at the station. Error bars are the standard errors. Different letters (a-f) indicate the significant differences ($P < 0.05$) in sampled stations during ebb tide, and significant differences ($P < 0.05$) during the flood tide are in brackets.

Downstream (i.e. stations S8-S9 in the three sampling periods) the DOM had only autochthonous origin (Fig. 5). The DOM at the stations S3-S7 in November, station S7 in April and stations S6 and S7 in August was a result of the combination of two sources. The FI values from stations S1 to S4 followed the order: November > August > April, while at stations S6-S7 the order changed to August > November > April. In addition, the average FI of station S8 and S9 during the flood tide was lower than that in the ebb tide because the autochthonous DOM in the downstream was diluted by salt seawater.

BIX, the freshness index (Morling et al., 2017), was used to assess the relative presence of the M fluorophore and the characteristic of autochthonous biological activity in the water (Huguet et al., 2009; Li et al., 2022). The average BIX showed decreasing trend from station S1 to S9 (Fig. 5). In the three sampling months, the BIX values at stations S1-S3 ranged from 0.86 to 1.53, indicating freshly DOM of biological/microbial origin (Table 2). However, protein-like materials were more prevalent in this reach (Gao et al., 2017). The lower BIX values at stations S7-S9 (i.e. 0.23–0.57), indicated as source water intrusions rather than autochthonous origin, because of the little amount of organic matter. The BIX values in November were higher than in April and August at stations S1-S6, while at

stations S7-S9 BIX in November, April and August were quite similar. Besides, there were no obvious pattern for the BIX changes between the ebb tide and flood tide at stations S8 and S9.

HIX implied the age of material and the recalcitrance within a natural system, measuring the complexity and the condensed aromatic nature of DOM compounds (Morling et al., 2017; Ohno et al., 2007). The HIX in the research area ranged from 0.66 to 3.85 and showed a decreasing trend from upstream to downstream (Table 2 and Fig. 5). Low HIX indicated the autochthonous fresh DOM of biological origin, plant biomass or animal manure generated in the whole reach (Huguet et al., 2009). Hereby, the characteristic of autochthonous DOM in the downstream was more obvious compared with that in the upstream. Besides, the HIX values during the flood tide slightly increased compared with those in the ebb tide, which indicated that the humification degree of seawater was higher than that of freshwater.

The concentration of FDOM ranged from 4.12 to 20.45 R. U. and decreased from station S1 to station S9 except S6 (Table 2 and Fig. 5). The FDOM concentration at station S6 was significantly higher compared with the similar location (i.e. S7), which was related to the domestic wastewater emission in the upstream of station S6 and thereby enhanced freshly

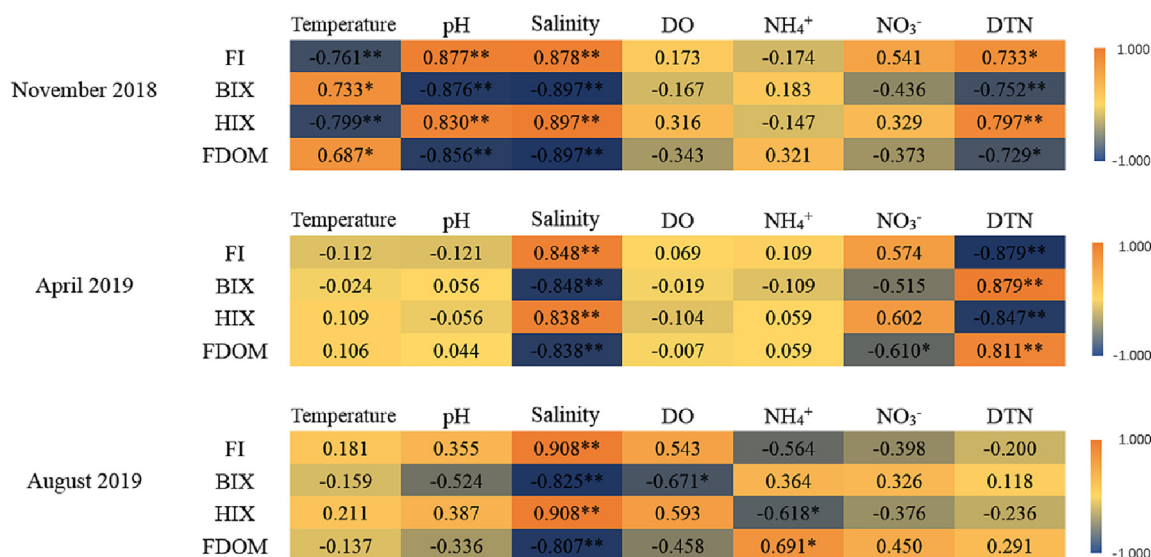


Fig. 6. Pearson and Spearman correlation analysis for DOM fluorescence indices and physicochemical properties in November 2018, April 2019 and August 2019. * Indicates significant correlation at the 0.05 level. ** Indicates significant correlation at the 0.01 level. Numbers with orange background belong to parameters with a positive relationship and numbers with blue background are associated with negatively correlated parameters.

produced microbial proteins (Parlanti et al., 2000; Wu et al., 2003; Zanardi-Lamardo et al., 2004). The concentration of protein-like FDOM increased with the bacterial biomass, resulting in the sharp increase of the FDOM concentration at S6 (Arai et al., 2018). Besides, the temporal change of the FDOM concentration was generally in the following order: November > April > August. While FDOM concentration at stations S5 and S6 were relatively similar during the three sampling periods. Additionally, there was no differences between the ebb tide and the flood tide in the downstream reach.

The Pearson's and Spearman's correlation analysis for DOM fluorescence indices and physicochemical properties are shown in Fig. 6. In November, the DOM fluorescence indices were significantly related to temperature, pH, salinity and DTN ($P < 0.05$). While in April, the DOM fluorescence indices were only significantly related to salinity and DTN ($P < 0.01$). Besides, NO₃⁻ negatively related to FDOM. In August, the salinity was the main factor influencing the DOM fluorescence indices ($P < 0.01$) and the highest salinity occurred in this month. Besides, NH₄⁺ and DO could affect some fluorescence indices to some extent. The correlation between FDOM and DO and DTN were found in Erhai Lake (Zhao et al., 2013; Zhao et al., 2019). However, in this study there was no relationship between FDOM and DO, and the salinity mainly affected the concentration of FDOM. Especially the DO in November and August were 6.81–7.50 and 5.50–6.93 mg·L⁻¹ with low variability. Whereas the salinity dominated the tidal reach. In addition, previous studies have shown that NH₄⁺ and NO₃⁻ could be photochemically produced or released from the DOM that have adsorbed NH₄⁺ or containing amino groups (Bronk et al., 2010; Kieber et al., 1999; Tarr et al., 2001; Yan et al., 2011). However, DTN in the research area was more important for the fluorescence indices compared with the NH₄⁺ and NO₃⁻ especially in November and April and higher DTN were determined in these two months. The higher DTN provided the enough nitrogen content, which could be used by bacteria to produce the DOM. Besides, the nitrogen pulses had direct and cascading effects on DOM composition (Goldberg et al., 2017). Hence, the FDOM was relatively higher in November and April with higher nitrogen.

4. Conclusions

Our field investigations showed that in nitrogen rich tidal river, salt intrusion and aquatic N speciation could play an important seasonal impact on the spatial distribution of DOM. The salinity and the main N species as well as the DOM characteristics revealed the existence of a clear spatiotemporal variability. The tyrosine-like proteins, tryptophan-like proteins or a

combination of the peak N and tryptophan-like fluorophore as well as the humic-like materials were the main DOM components in the estuarine area. The salinity played the most important role for the DOM distribution. The fluorescence levels under high salinity conditions were more dispersed than those in the upstream reach, and the fluorescence intensities during the flood tide were lower than those during the ebb tide. Besides, the higher DTN levels significantly related to the DOM fluorescence indices. The FI and HIX increased and BIX and FDOM decreased when the salinity increase. The rich nitrogen sources could stimulate the DOM production. Taken together, our results ascertain the possible effect of salinity intrusion and aquatic N level on the distribution and change of DOM in estuarine areas. This knowledge is critical for guiding management efforts aimed at tracing the DOM pollution and improving water quality in estuaries.

CRedit authorship contribution statement

Rongrong Xie: Conceptualization, Methodology, Writing - review & editing, Visualization, Supervision.

Jiabing Qi: Data curation, performed the analysis, Writing- Original draft preparation.

Chengchun Shi: Resources, Funding acquisition.

Peng Zhang: Methodology.

Rulin Wu: Investigation, Data curation.

Liabing Li: Investigation, Resources.

Joanna J. Waniek: Writing - review & editing, Supervision.

Data availability

Data will be made available on request.

Declaration of competing interest

The authors declare that they have no known competing financial interests or personal relationships that could have appeared to influence the work reported in this paper.

Acknowledgments

This work was partially supported by the National Natural Science Foundation of China (42007343) and the Fujian Provincial Natural Science Foundation (2021J01195). Besides, I extend my appreciation and thanks towards my co-workers that contributed to the field surveys, with especial

thanks to Prof. Zuliang Chen. We are also grateful to the journal experts for their valuable comments on this paper.

Appendix A. Supplementary data

Supplementary data to this article can be found online at <https://doi.org/10.1016/j.scitotenv.2023.163251>.

References

- Adey, W.H., Loveland, K., 2007. Chapter 22-estuaries: ecosystem modeling and restoration. *Dynamic Aquaria*. 3, pp. 405–441.
- Aitkenhead-Peterson, J.A., McDowell, W.H., Neff, J.C., 2003. Sources, production, and regulation of allochthonous dissolved organic matter inputs to surface waters. In: Findlay, S.E.G., Sinsabaugh, R.L. (Eds.), *Aquatic Ecosystems: Interactivity of Dissolved Organic Matter*. Academic Press, Burlington, pp. 25–70.
- Andersen, C.M., Bro, R., 2003. Practical aspects of PARAFAC modeling of fluorescence excitation-emission data. *J. Chemom.* 17, 200–215.
- Andersson, C.A., Bro, R., 2000. The N-way toolbox for MATLAB. *Chemom. Intell. Lab. Syst. S.* 52, 1–4.
- Arai, K., Wada, S., Shimotori, K., Omori, Y., Hama, T., 2018. Production and degradation of fluorescent dissolved organic matter derived from bacteria. *J. Oceanogr.* 74, 39–52.
- Berg, S.M., Mooney, R.J., McConville, M.B., McIntyre, P.B., Remucal, C.K., 2021. Seasonal and spatial variability of dissolved carbon concentration and composition in Lake Michigan tributaries. *J. Geophys. Res. Biogeosci.* 126, e2021JG006449.
- Birdwell, J.E., Engel, A.S., 2010. Characterization of dissolved organic matter in cave and spring waters using UV-vis absorbance and fluorescence spectroscopy. *Org. Geochem.* 41, 270–280.
- Bricker, S.B., Longstaff, B., Dennison, W., Jones, A., Boicourt, K., Wicks, C., Woerner, J., 2008. Effects of nutrient enrichment in the nation's estuaries: a decade of change. *Harmful Algae* 8, 21–32.
- Bridgeman, J., Bieroza, M., Baker, A., 2011. The application of fluorescence spectroscopy to organic matter characterisation in drinking water treatment. *Rev. Environ. Sci. Biotechnol.* 10, 277–290.
- Bronk, D.A., Roberts, Q.N., Sanderson, M.P., Canuel, E.A., Hatcher, P.G., Mesfioui, R., Filippino, K.C., Mulholland, M.R., Love, N.G., 2010. Effluent organic nitrogen (EON): bioavailability and photochemical and salinity-mediated release. *Environ. Sci. Technol.* 44, 5830–5835.
- Chen, B., Kim, Y., Westerhoff, P., 2011. Occurrence and treatment of wastewater-derived organic nitrogen. *Water Res.* 45, 4641–4650.
- Chen, J., LeBoeuf, E.J., Dai, S., Gu, B., 2003a. Fluorescence spectroscopic studies of natural organic matter fractions. *Chemosphere* 50, 639–647.
- Chen, W., Westerhoff, P., Leenheer, J.A., Booksh, K., 2003b. Fluorescence excitation-emission matrix regional integration to quantify spectra for dissolved organic matter. *Environ. Sci. Technol.* 37, 5701–5710.
- Chen, M., Nam, S.I., Kim, J.H., Kwon, Y.J., Hong, S., Jung, J., Shin, K.H., Hur, J., 2017. High abundance of protein-like fluorescence in the Amerasian Basin of Arctic Ocean: potential implication of a fall phytoplankton bloom. *Sci. Total Environ.* 599, 355–363.
- Chu, J., Luo, C., Wang, H., Liao, Z., 2022. Insights into the associations between optical and molecular signatures of dissolved organic matter from urban stormwater runoff. *Environ. Sci. Technol.* 2, 339–348.
- Coble, P.G., 2007. Marine optical biogeochemistry: the chemistry of ocean color. *Chem. Rev.* 107, 402–418.
- Coble, P.G., Del Castillo, C.E., Avril, B., 1998. Distribution and optical properties of CDOM in the Arabian Sea during the 1995 Southwest Monsoon. *Deep-Sea Res. II Top. Stud. Oceanogr.* 45, 2195–2223.
- Cory, R.M., McKnight, D.M., 2005. Fluorescence spectroscopy reveals ubiquitous presence of oxidized and reduced quinones in dissolved organic matter. *Environ. Sci. Technol.* 39, 8142–8149.
- Czerwionka, K., Makinia, J., Pagilla, K.R., Stensel, H.D., 2012. Characteristics and fate of organic nitrogen in municipal biological nutrient removal wastewater treatment plants. *Water Res.* 46, 2057–2066.
- Del Castillo, C.E., Coble, P.G., Morell, J.M., Lopez, J.M., Corredor, J.E., 1999. Analysis of the optical properties of the Orinoco River plume by absorption and fluorescence spectroscopy. *Mar. Chem.* 66, 35–51.
- Des, M., Fernández-Nóvoa, D., deCastro, M., Gómez-Gesteira, J.L., Sousa, M.C., Gomez-Gesteira, M., 2021. Modeling salinity drop in estuarine areas under extreme precipitation events within a context of climate change: effect on bivalve mortality in Galician Rias Baixas. *Sci. Total Environ.* 790, 148147.
- DiLorenzo, J.L., Filadelfo, R.J., Surak, C.R., Litwack, H.S., Gunawardana, V.K., Najarian, T., 2004. Tidal variability in the water quality of an urbanized estuary. *Estuar. Coasts* 27, 851–860.
- Elliott, S., Lead, J.R., Baker, A., 2006. Characterisation of the fluorescence from freshwater, planktonic bacteria. *Water Res.* 40, 2075–2083.
- Fisher, T.R., Rochelle-Newall, E.J., 2002. Production of chromophoric dissolved organic matter fluorescence in marine and estuarine environments: an investigation into the role of phytoplankton. *Mar. Chem.* 77, 7–21.
- Gao, J., Liang, C., Shen, G., Lv, J., Wu, H., 2017. Spectral characteristics of dissolved organic matter in various agricultural soils throughout China. *Chemosphere* 176, 108–116.
- Goldberg, S.J., Nelson, C.E., Viviani, D.A., Shulze, C.N., Church, M.J., 2017. Cascading influence of inorganic nitrogen sources on DOM production, composition, lability and microbial community structure in the open ocean. *Environ. Microbiol.* 19, 3450–3464.
- Goldman, J.H., Rounds, S.A., Needoba, J.A., 2012. Applications of fluorescence spectroscopy for predicting percent wastewater in an urban stream. *Environ. Sci. Technol.* 46, 4374–4381.
- Graeber, D., Gelbrecht, J., Pusch, M.T., Anlanger, C., Schiller, D.V., 2012. Agriculture has changed the amount and composition of dissolved organic matter in central European headwater streams. *Sci. Total Environ.* 438, 435–446.
- Henderson, R.K., Baker, A., Murphy, K.R., Hamblly, A., Stuetz, R.M., Khan, S.J., 2009. Fluorescence as a potential monitoring tool for recycled water systems: a review. *Water Res.* 43, 863–881.
- HJ 493, 2009. Water quality- technical regulation of the preservation and handling of samples. <http://kjs.mee.gov.cn/hjbhbz/bzwb/jcfbz/200910/W020111114540735543139.pdf>.
- HJ 535, 2009. Water quality- determination of ammonia nitrogen-Nessler's reagent spectrophotometry. http://english.mee.gov.cn/Resources/standards/water_environment/method_standard2/201010/t20101027_196755.shtml.
- HJ 636, 2012. Water quality- determination of total nitrogen-alkaline potassium persulfate digestion UV spectrophotometric method. http://english.mee.gov.cn/Resources/standards/water_environment/method_standard2/201206/t20120618_231805.shtml.
- HJ/T 346, 2007. Water quality- determination of nitrate-nitrogen- ultraviolet spectrophotometry. http://english.mee.gov.cn/Resources/standards/water_environment/method_standard2/200807/t20080704_125017.shtml.
- Hudson, N., Baker, A., Ward, D., Reynolds, D.M., Brunsdon, C., Carliell-Marquet, C., Browning, S., 2008. Can fluorescence spectrometry be used as a surrogate for the Biochemical Oxygen Demand (BOD) test in water quality assessment? An example from South West England. *Sci. Total Environ.* 391, 149–158.
- Huguet, A., Vacher, L., Relexans, S., Saubusse, S., Froidefond, J.M., Parlanti, E., 2009. Properties of fluorescent dissolved organic matter in the Gironde Estuary. *Org. Geochem.* 40, 706–719.
- Kalbitz, K., Geyer, S., Geyer, W., 2000. A comparative characterization of dissolved organic matter by means of original aqueous samples and isolated humic substances. *Chemosphere* 40, 1305–1312.
- Kennish, M.J., 2016. Anthropogenic impacts. In: Kennish, M.J. (Ed.), *Encyclopedia of Estuaries*, Encyclopedia of Earth Sciences Series. Springer, Dordrecht, The Netherlands, pp. 29–35.
- Kieber, R.J., Li, A., Seaton, P.J., 1999. Production of nitrite from the photodegradation of dissolved organic matter in natural waters. *Environ. Sci. Technol.* 33, 993–998.
- Li, Y., Zhou, Y., Zhou, L., Zhang, Y., Xu, H., Jang, K.S., Kothawala, D.N., Spencer, R., Jeppesen, E., Brookes, J.D., Davidson, T.A., Wu, F., 2022. Changes in water chemistry associated with rainstorm events increase carbon emissions from the inflowing river mouth of a major drinking water reservoir. *Environ. Sci. Technol.* 56, 16494–16505.
- Lin, Y., Hu, E., Sun, C., Li, M., Gao, L., Fan, L., 2023. Using fluorescence index (FI) of dissolved organic matter (DOM) to identify non-point source pollution: the difference in FI between soil extracts and wastewater reveals the principle. *Sci. Total Environ.* 862, 160848.
- Liu, S., He, Z., Tang, Z., Liu, L., Hou, J., Li, T., Zhang, Y., Shi, Q., Giesy, J.P., Wu, F., 2020. Linking the molecular composition of autochthonous dissolved organic matter to source identification for freshwater lake ecosystems by combination of optical spectroscopy and FT-ICR-MS analysis. *Sci. Total Environ.* 703, 134764.
- Lu, Y., Shang, P., Chen, S., Du, Y., Bonizzoni, M., Ward, A.K., 2021. Discharge and temperature controls of dissolved organic matter (DOM) in a forested coastal plain stream. *Water* 13, 2919.
- Mayer, L.M., Schick, L.L., Loder III, T.C., 1999. Dissolved protein fluorescence in two Maine estuaries. *Mar. Chem.* 64, 171–179.
- McKnight, D.M., Boyer, E.W., Westerhoff, P.K., Doran, P.T., Kulbe, T., Andersen, D.T., 2001. Spectrofluorometric characterization of dissolved organic matter for indication of precursor organic material and aromaticity. *Limnol. Oceanogr.* 46, 38–48.
- Meng, F., Huang, G., Yang, X., Li, Z., Li, J., Cao, J., Wang, Z., Sun, L., 2013. Identifying the sources and fate of anthropogenically impacted dissolved organic matter (DOM) in urbanized rivers. *Water Res.* 47, 5027–5039.
- Mesfioui, R., Love, N.G., Bronk, D.A., Mulholland, M.R., Hatcher, P.G., 2012. Reactivity and chemical characterization of effluent organic nitrogen from wastewater treatment plants determined by fourier transform ion cyclotron resonance mass spectrometry. *Water Res.* 46, 622–634.
- Morling, K., Herzsprung, P., Kamjunke, N., 2017. Discharge determines production of, decomposition of and quality changes in dissolved organic carbon in pre-dams of drinking water reservoirs. *Sci. Total Environ.* 577, 329–339.
- Murphy, K.R., Stedmon, C.A., Waite, T.D., Ruiz, G.M., 2008. Distinguishing between terrestrial and autochthonous organic matter sources in marine environments using fluorescence spectroscopy. *Mar. Chem.* 108, 40–58.
- Nagata, T., 2000. Production mechanisms of dissolved organic matter. In: Kirchman, D.L. (Ed.), *Microbial Ecology of the Oceans*, Wiley Series in Ecological and Applied Microbiology. Wiley-Liss, pp. 121–152.
- Nascimento, Á., Biguino, B., Borges, C., Cereja, R., Cruz, J.P., Sousa, F., Dias, J., Brotas, V., Palma, C., Brito, A.C., 2021. Tidal variability of water quality parameters in a mesotidal estuary (Sado Estuary, Portugal). *Sci. Rep.* 11, 1–17.
- Nguyen, T.T.M., Yu, X., Pu, L., Xin, P., Zhang, C., Barry, D.A., Li, L., 2020. Effects of temperature on tidally influenced coastal unconfined aquifers. *Water Resour. Res.* 56, 1–17.
- Ogawa, H., Amagai, Y., Koike, I., Kaiser, K., Benner, R., 2001. Production of refractory dissolved organic matter by bacteria. *Science* 292, 917–920.
- Ohno, T., Chorover, J., Omoike, A., Hunt, J., 2007. Molecular weight and humification index as predictors of adsorption for plant-and manure-derived dissolved organic matter to goethite. *Eur. J. Soil Sci.* 58, 125–132.
- Parlanti, E., Wörz, K., Geoffroy, L., Lamotte, M., 2000. Dissolved organic matter fluorescence spectroscopy as a tool to estimate biological activity in a coastal zone submitted to anthropogenic inputs. *Org. Geochem.* 31, 1765–1781.
- Peiris, R.H., Budman, H., Moresoli, C., Legge, R.L., 2011. Identification of humic acid-like and fulvic acid-like natural organic matter in river water using fluorescence spectroscopy. *Water Sci. Technol.* 63, 2427–2433.

- Pesaranghader, A., Matwin, S., Sokolova, M., Beiko, R.G., 2016. simDEF: definition-based semantic similarity measure of gene ontology terms for functional similarity analysis of genes. *Bioinformatics* 32, 1380–1387.
- Rodríguez, F.J., Schlenger, P., García-Valverde, M., 2014. A comprehensive structural evaluation of humic substances using several fluorescence techniques before and after ozonation. Part I: structural characterization of humic substances. *Sci. Total Environ.* 476, 718–730.
- Rodríguez-Vidal, F.J., García-Valverde, M., Ortega-Azabache, B., González-Martínez, Á., Bellido-Fernández, A., 2020. Characterization of urban and industrial wastewaters using excitation-emission matrix (EEM) fluorescence: searching for specific fingerprints. *J. Environ. Manag.* 263, 110396.
- Sirivedhin, T., Gray, K.A., 2005. Part I. Identifying anthropogenic markers in surface waters influenced by treated effluents: a tool in potable water reuse. *Water Res.* 39, 1154–1164.
- Song, X., Zhao, M., Chen, A., Xie, X., Yang, H., Zhang, S., Wei, Z., Zhao, Y., 2022. Effects of input of terrestrial materials on photodegradation and biodegradation of DOM in rivers: the case of Heilongjiang River. *J. Hydrol.* 609, 127792.
- Stedmon, C.A., Bro, R., 2008. Characterizing dissolved organic matter fluorescence with parallel factor analysis: a tutorial. *Limnol. Oceanogr. Methods* 6, 572–579.
- Stedmon, C.A., Markager, S., 2005. Resolving the variability in dissolved organic matter fluorescence in a temperate estuary and its catchment using PARAFAC analysis. *Limnol. Oceanogr.* 50, 686–697.
- Stedmon, C.A., Markager, S., Bro, R., 2003. Tracing dissolved organic matter in aquatic environments using a new approach to fluorescence spectroscopy. *Mar. Chem.* 82, 239–254.
- Stedmon, C.A., Thomas, D.N., Granskog, M., Kaartokallio, H., Papadimitriou, S., Kuosa, H., 2007. Characteristics of dissolved organic matter in Baltic coastal sea ice: allochthonous or autochthonous origins? *Environ. Sci. Technol.* 41, 7273–7279.
- Tarr, M.A., Wang, W., Bianchi, T.S., Engelhaupt, E., 2001. Mechanisms of ammonia and amino acid photoproduction from aquatic humic and colloidal matter. *Water Res.* 35, 3688–3696.
- Wagner, K., Bengtsson, M.M., Besemer, K., Sieczko, A., Burns, N.R., Herberg, E.R., Battin, T.J., 2014. Functional and structural responses of hyporheic biofilms to varying sources of dissolved organic matter. *Appl. Environ. Microbiol.* 80, 6004–6012.
- Wang, Z., Cao, J., Meng, F., 2015. Interactions between protein-like and humic-like components in dissolved organic matter revealed by fluorescence quenching. *Water Res.* 68, 404–413.
- Wen, Y., Shan, B., Zhang, W., 2021. Nitrogen distribution and inorganic nitrogen diffusion flux in a shallow lake during the low temperature period: a case study of the Baiyangdian lake. *Environ. Sci.* 42, 2839–2847 (In Chinese).
- Wen, Z., Shang, Y., Song, K., Liu, G., Hou, J., Lyu, L., Tao, H., Li, S., He, C., Shi, Q., He, D., 2022. Composition of dissolved organic matter (DOM) in lakes responds to the trophic state and phytoplankton community succession. *Water Res.* 224, 119073.
- Wickland, K.P., Neff, J.C., Aiken, G.R., 2007. Dissolved organic carbon in Alaskan boreal forest: sources, chemical characteristics, and biodegradability. *Ecosystems* 10, 1323–1340.
- Wilson, A.M., 2005. Fresh and saline groundwater discharge to the ocean: a regional perspective. *Water Resour. Res.* 41, 1–11.
- Wu, F., Tanoue, E., Liu, C., 2003. Fluorescence and amino acid characteristics of molecular size fractions of DOM in the waters of Lake Biwa. *Biogeochemistry* 65, 245–257.
- Wünsch, U.J., Bro, R., Stedmon, C.A., Wenig, P., Murphy, K.R., 2019. Emerging patterns in the global distribution of dissolved organic matter fluorescence. *Anal. Methods* 11, 888–893.
- Xie, R., Pang, Y., Luo, B., Li, J., Wu, C., Zheng, Y., Sun, Q., Zhang, P., Wang, F., 2017. Spatiotemporal variability in salinity and hydraulic relationship with salt intrusion in the tidal reaches of the Minjiang River, Fujian province, China. *Environ. Sci. Pollut. Res.* 24, 11847–11855.
- Xie, R., Rao, P., Pang, Y., Shi, C., Li, J., Shen, D., 2020. Salt intrusion alters nitrogen cycling in tidal reaches as determined in field and laboratory investigations. *Sci. Total Environ.* 729, 138803.
- Xie, R., Zhen, L., Wu, X., Li, J., 2023. Isotopic compositions (δD , $\delta^{18}O$) and end-member mixing for the control interface in a complex tidal region. *Sci. Total Environ.* 866, 161438.
- Yamashita, Y., Jaffé, R., Maie, N., Tanoue, E., 2008. Assessing the dynamics of dissolved organic matter (DOM) in coastal environments by excitation emission matrix fluorescence and parallel factor analysis (EEM-PARAFAC). *Limnol. Oceanogr.* 53, 1900–1908.
- Yan, C., Wang, S., Xue, N., Jiao, L., Jin, X., 2011. Effects of submerged plants on fluorescent characteristics of DOM in sediments under different doses of NH_3-N . *Environ. Sci. Res.* 24, 740–747 (In Chinese).
- Yang, F., Song, G., Massicotte, P., Wei, H., Xie, H., 2020. Depth-resolved photochemical lability of dissolved organic matter in the western tropical Pacific Ocean. *J. Geophys. Res. Biogeosci.* 125, e2019JG005425.
- Zanardi-Lamardo, E., Moore, C.A., Zika, R.G., 2004. Seasonal variation in molecular mass and optical properties of chromophoric dissolved organic material in coastal waters of south-west Florida. *Mar. Chem.* 89, 37–54.
- Zhang, T., Lu, J., Ma, J., Qiang, Z., 2008. Fluorescence spectroscopic characterization of DOM fractions isolated from a filtered river water after ozonation and catalytic ozonation. *Chemosphere* 71, 911–921.
- Zhang, Y., Yin, Y., Feng, L., Zhu, G., Shi, Z., Liu, X., Zhang, Y., 2011. Characterizing chromophoric dissolved organic matter in Lake Tianmuhu and its catchment basin using excitation-emission matrix fluorescence and parallel factor analysis. *Water Res.* 45, 5110–5122.
- Zhang, X., Nie, L., Gao, H., Yu, H., Liu, D., 2023. Applying second derivative synchronous fluorescence spectroscopy combined with Gaussian band fitting to trace variations of DOM fractions along an urban river. *Ecol. Indic.* 146, 109872.
- Zhao, H., Wang, S., Jiao, L., Yang, S., Xu, S., 2013. Space-time evolution trends of water nitrogen in Lake Erhai. *China Environ. Sci.* 33, 874–880 (In Chinese).
- Zhao, H., Li, Y., Wang, S., Jiao, L., Zhang, L., 2019. Fluorescence characteristics of DOM in overlying water of Erhai Lake and its indicative of eutrophication. *Spectrosc. Spectr. Anal.* 39, 3888–3896 (In Chinese).
- Zheng, C., Zeng, C., Chen, Z., Lin, M., 2006. A study on the changes of landscape pattern of estuary wetlands of the Minjiang River. *Wetland Sci.* 4, 29–34 (In Chinese).
- Zsolnay, A., Baigar, E., Jimenez, M., Steinweg, B., Saccomandi, F., 1999. Differentiating with fluorescence spectroscopy the sources of dissolved organic matter in soils subjected to drying. *Chemosphere* 38, 45–50.